INTERNATIONAL JOURNAL OF
ENERGY AND ENVIRONMENT

Volume 1, Issue 6, 2010 pp.937-952
Journal homepage: www.IJEE. IEEFoundation.org

CFD for hydrodynamic efficiency and design optimization of key elements of SHP

Ana Pereira, Helena M. Ramos

Civil Engineering Department and CEHIDRO, Instituto Superior Técnico, Technical University of Lisbon, Av. Rovisco Pais, 1049-001, Lisbon, Portugal.

Abstract
This paper aims to study how the flow behaves in key elements of small hydropower plants (SHP) which should be well designed in order to achieve properly the best hydraulic and energy efficiency.
There are some hydrodynamic and structural fundaments that all hydro circuits design has to follow, and there are other aspects that vary from design to the flow behavior. The variables that influence the hydro systems design are related with performance, technical, operational and environmental aspects. For instance, design discharge, produced energy, intakes and outlets geometry are some of the technical variables.
The components of SHP design should be characterized by a balance between hydraulic, structural, operational and environment efficiency and economic issues. To improve the hydraulic efficiency is necessary information concerning with hydrodynamic flow behavior. The knowledge in this area is still insufficient since the hydrodynamic flow patterns, in some key elements of hydraulic circuits of SHP are quite complex. Therefore this paper uses an advanced computational fluid dynamic (CFD) model for flow simulation, with the aim to improve the behavior comprehension enabling the identification of parameters' variation which influences the performance efficiency of those components in the design criteria of such SHP.
Since the inefficiency and the unsafe operating conditions are normally associated to separated flow zones, vorticity development, macro turbulence intensity, pressure gradients, shear stress increase, this paper intends to analyze causes and consequences of the flow behavior. Among these concerns it is possible to identify induced problems, such as vibrations, resonance effects, ruptures or collapses, cavitation, water column separation, significant friction losses, vortices and regions of reversed flow.
Copyright © 2010 International Energy and Environment Foundation - All rights reserved.

Keywords: CFD analysis, SHP, Design optimization, Hydraulic circuit.

1. Introduction

1.1 Flow control valves

Hydraulic systems are composed of a set of pipes, valves and other hydromechanical equipments necessary for adequate operational management, control and safety.

Valves are devices of great importance in the operation of hydro systems, in particular, when is necessary to control the flow [1, 2]. There are different types of valves in order to perform these functions. Depending on the shutter movement, the valves can be classified into two groups:
- Valves with linear motion (e.g., globe; wedge; shears, needle, diaphragm);
- Valves with angular motion (spherical; butterfly).

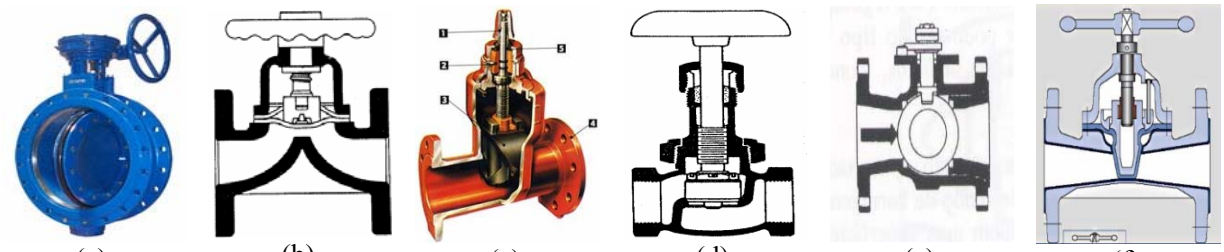

(a) (b) (c) (d) (e) (f)

Figure 1. Different types of control valves

The butterfly valve, (Figure 1a) is often used in water systems, under low hydraulic loads. They are valves suited for emergency shut-off, more specifically, for safety valves with overspeed closing disposal. The diaphragm valves are characterized by having a flexible membrane (diaphragm) whose periphery is fixed in the body of the valve (Figure 1b). As for membrane valve (Figure 1f), it works by pressing one side of the membrane through the actuator, restricting the passage of the flow. This type of valve is used, preferably, in situations of hostile operation. The spherical valves, the wedge (Figure 1c) and shears are the most suitable for the task of stopping the flow. The globe valves (Figure 1d) have a great use in automatic control of pressure and flow. They can present various shutter types and regulation hydraulic systems. Due to the pathway that the liquid makes inside, these valves have a large loss of hydraulic load, even in situations of total openness. The spherical valves (Figure 1e) are, preferably, used at systems with high hydraulic load or for quick flow cuts under high pressure situations. These valves when fully opened induce a low loss of hydraulic load.

1.2 Vortex formation

The consequences of vortex formation and development can be the air entrance into the hydraulic circuit, flow circulation, separation zones and pressure and flow velocity variation [1]. There are three different types of vortices, namely forced vortex, free vortex and mixed vortex. On a forced vortex the water has a rotation movement around an axis as a solid body, which is caused by an external force, on which the tangential velocity is proportional to the distance from the axis, where the flow is rotational. When the actuation of the forces finishes, the rotation movement around the axis occurs freely inducing a free vortex, on which the flow velocity is inversely proportional to the distance from the axis, with an irrotational movement. The Euler number that represents the drop pressure by the increasing of the velocity is an adequate parameter to describe the vortex development. The mixed vortex is a combination of a forced vortex near the centre of rotation and a free vortex at the main body.

1.3 Intakes

The vortex, which exists at intake pipes, is considered a free vortex with air dragging [2, 3, 4]. The free vortex can be classified a surface or a submerged type. From the stability point of view they can be identified as steady, unsteady or intermittent category and the circulation intensity can be organized in six levels, from weak to strong (Figure 2).

 ©2010 International Energy & Environment Foundation. All rights reserved.

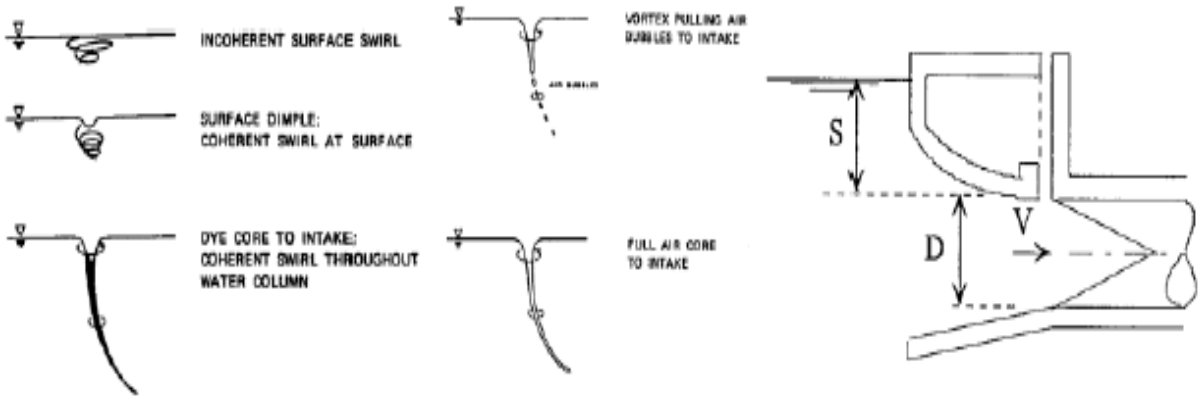

Figure 2. Different types of vortex at a typical SHP intake

As main causes for vortex formation can be referred the eccentric orientation of the intake inlet relative to a symmetric approach, asymmetric approach flow conditions, unfavorable effects of obstructions such as offsets, piers or dividing walls, non-uniform velocity distribution caused by boundary layer separation, wind action in the flow surface, wakes or counter currents and the insufficient intake submergence.
The consequences of vortex formation at intakes are air, swirl and even solid materials dragged into the intake conveyance hydraulic circuit which in turn induces unfavorable hydrodynamic impact on the operation and performance of turbines, and can cause dangerous hydropneumatic effects, such as noise and vibrations.

1.4 Draft tube and tailrace

Another challenge is to understand the hydrodynamic of the flow through a draft tube and a tailrace of a SHP [5, 6]. Operational conditions have significant influence on the turbine efficiency, particularly when those conditions are out of the best efficiency point (BEP).

Figure 3. Change of the runner speed and the frequency of vortex at the draft tube of a Francis turbine

One of the most important concerns on turbine runner and blades design is to guarantee a uniform flow to the draft tube entrance in non-disturbed conditions. The draft tube has a geometrical complexity resulting of changes on cross-section shape and direction in order to transform the flow kinetic energy into downstream potential energy position. In this region the flow presents large local pressure gradients, intense longitudinal vortices and regions of reversal flow (Figure 3).
Disturbed flow entrance at the draft tube may cause flow reversal downstream of the runner with flow recirculation, formation of rope vortices, cavitation phenomena, which induce considerable efficiency

 ©2010 International Energy & Environment Foundation. All rights reserved.

losses, dangerous pressure fluctuations, which can be propagated into the entire penstock. Thus poor inflow conditions may cause unfavorable hydrodynamic flow behavior.
Hence, this paper presents CFD simulations on which the effects on efficiency of SHP at the intake and at the tailrace resulting from changes on solid element configuration are analyzed in order to define the best geometries that can improve the system performance [7].

1.5 Measures and design criteria

The main advantages of reducing the turbulence and vortex intensity are related with the consequent discharge and head increase. This study evaluates effectiveness of using adequate valve design (type, opening degree and diameter), anti-vortex devices such as baffles (vertical walls) or vanes, modifying the shape of flow approach area, to eliminate approach flow non-uniformities creating a good inflow approximation, removing sharp singularities, modifying intake and outlet geometries to lengthen uniform streamlines and to guarantee the minimum submergence or the admissible suction head in reducing the vortex and flow circulation effects at intakes, draftubes and tailraces and turbine operation [8, 9]. To avoid separated flow zones, with non uniform velocity distribution and to minimize head losses, changes on inlet and outlet walls shape design are considered. To decrease the free vortex with air dragging intensity, this study also evaluates the advantages of keep the water level above the critical submergence level, in order to always guarantee the intake inlet submergence.
The hydrodynamic flow configuration and the design of special hydraulic structures and devices, such as control discharge structures and valves to control the flow behavior and regulate the pressure are also analyzed.

2. Mathematical approach

Although the Navier-Stokes equations have a limited number of known analytical solutions, they are adequate for the flow computational model, by numerical approach of computational fluid dynamics. The CFD model (FloEFD) solves the Navier-Stokes equations, which are formulations of mass, momentum and energy conservation laws for fluid flows. The equations are supplemented by fluid state equations defining the nature of the fluid, and by empirical dependencies of fluid density, viscosity and thermal conductivity on temperature [7, 10, 11].
The Navier Stokes equations are presented by equations (1) for incompressible flows, where these equations are based on differential equations of linear momentum for a Newtonian fluid with constants density and viscosity.

$$\begin{aligned}
\rho g_x - \frac{dp}{dx} + \mu\left(\frac{\partial^2 u}{\partial x^2} + \frac{\partial^2 u}{\partial y^2} + \frac{\partial^2 u}{\partial z^2}\right) &= \rho \frac{du}{dt} \\
\rho g_y - \frac{dp}{dy} + \mu\left(\frac{\partial^2 v}{\partial x^2} + \frac{\partial^2 v}{\partial y^2} + \frac{\partial^2 v}{\partial z^2}\right) &= \rho \frac{dv}{dt} \\
\rho g_z - \frac{dp}{dz} + \mu\left(\frac{\partial^2 w}{\partial x^2} + \frac{\partial^2 w}{\partial y^2} + \frac{\partial^2 w}{\partial z^2}\right) &= \rho \frac{dw}{dt}
\end{aligned} \tag{1}$$

where: ρ: volumetric mass (kg/m^3); g: acceleration of gravity (m/s^2); p: pressure (Pa); μ: dynamic viscosity (kg/(ms)); u, v, w: velocity components for each moving fluid particle, depending on x, y, z coordinates for a given t instant (m/s).

The incompressible fluid flow behavior is determined by the velocity and pressure variables and their variations in time and space. In equations (1), that allow to get pressure and velocity fields, the velocity components at each point x, y, z are vector fields and the pressures.
Most of the flows that occur at hydraulic circuits are turbulent, and this CFD model allows the numerical modeling of both laminar and turbulent conditions. The turbulent flows occur for high values of Reynolds number, given y the equation (2).

 ©2010 International Energy & Environment Foundation. All rights reserved.

$$R_e = \frac{\rho U D}{\mu} \quad (2)$$

where: D : conduit diameter (m).

When the flow is turbulent the variables present at each instant random fluctuations. A fluid under to low pressures can reach the vapor pressure at the local temperature leading to the formation of vaporous cavities. The fluid undergoes a phase change and cavities filled with fluid vapor and other dissolved gases are formed. When analyzing areas of flow conditions that leads the occurrence of cavitation, this CFD model, uses an homogeneous equilibrium model of cavitation in water

3. Results analysis

3.1 Hydrodynamic flow behavior through flow control valves

The flow was simulated through flow control valves for different valve closure positions [12]. For valves with actuator's angular movement (e.g. ball valve) the flow was simulated for different valve opening angles. The angle of valve opening is measured in relation to the position of fully closed valve. For valves with actuator's linear movement (e.g. globe valve) the flow was simulated for different opening percentages. The variation of valve head loss coefficient with valve closure position was obtained. This variation shows the energy dissipation induced by the valve in the flow for different valve opening positions.

3.1.1 Ball valve

The first step was to build the ball valve geometry model. Two pipe branches of equal length and diameter to the valve size were connected at upstream and downstream of the ball valve geometry model. Concerning to the energy dissipation induced by the ball valve, the values shown in Table 1 and in Graph 1 were obtained. Head losses are associated to the opened valve position. Thus the lower the opening angle the lower the pressure downstream of the valve which may lead to cavitation occurrence.

Table 1. Head loss and local head loss coefficient values for different ball valve opening angles

	Ball valve opening angle (°)					
	20	40	45	60	80	90
ΔH (m)	1300,25	24,28	11,13	2,46	0,48	0,01
Kv (-)	180,80	13,62	8,16	3,17	0,84	0,02

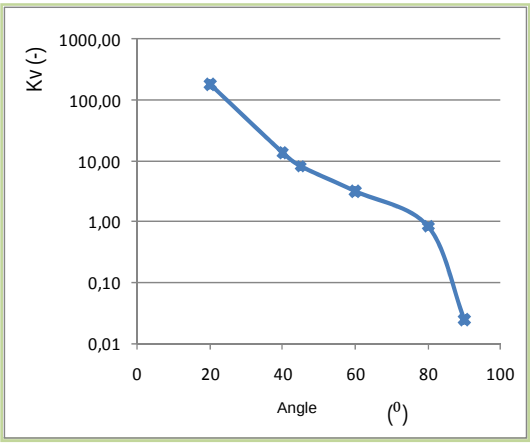

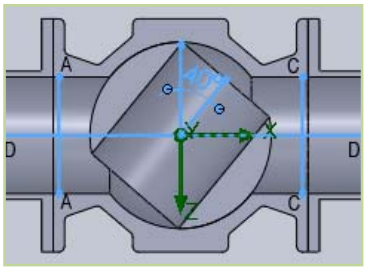

Graph 1. Ball valve local head loss coefficient K_v variation with the respective opening angle

 ©2010 International Energy & Environment Foundation. All rights reserved.

From velocity vector distribution, represented in Figure 4, can be concluded that the flow trajectories converge upstream of the valve which can lead to flow separation in the same region and to rotational movement with high turbulence inside the valve. Downstream the valve the velocity vector distribution shows a separation flow zone where occur strong vorticity with high turbulence intensity associated, which leads to local flow energy dissipation. As a result of this dissipation there is negative pressure downstream of the valve which contributes to the cavitation occurrence in this region. The major part of the pressure loss occurs at the closure outlet.

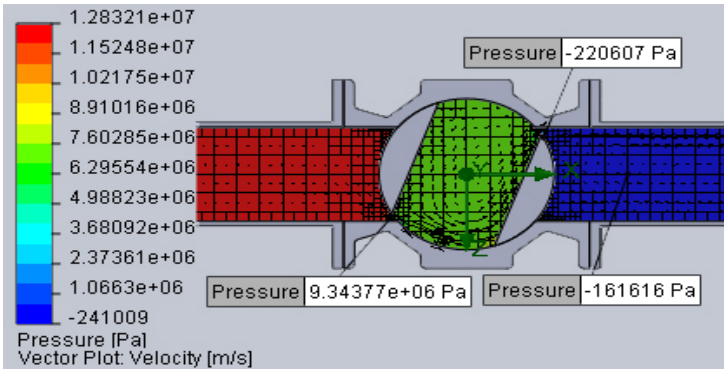

Figure 4. Ball valve opening angle of 20º - pressure distribution in a longitudinal section of a ball valve

Figure 5 shows the cavitation occurrence for a ball valve opening angle of 20º. Immediately downstream of the valve high vapor volume fraction values and low density of the mixture of water vapor, other dissolved gases in the water body and water values are verified. The pressure values increase again in the pipe downstream of the valve, therefore the vapor volume fraction values decrease again towards downstream and the density values of the mixture of water vapor, other dissolved gases and water increase again in the same direction. Both the water vapor density as the other dissolved gases density is lower than the water density, so that when these gases are dissolved in the water body there is a gas-water mixture of density lower than water density. The vapor volume fraction is the ratio between water vapor and other dissolved gases volume and the water volume in the gas-water mixture. Thus it is concluded that high vapor volume fraction values and low gas-water mixture density values indicate the presence of vapor bubbles in water body that are associated to the cavitation occurrence. The occurrence of this phenomenon in valves has strong influence in valve local head loss coefficient $K_v(-)$ values and in its security.

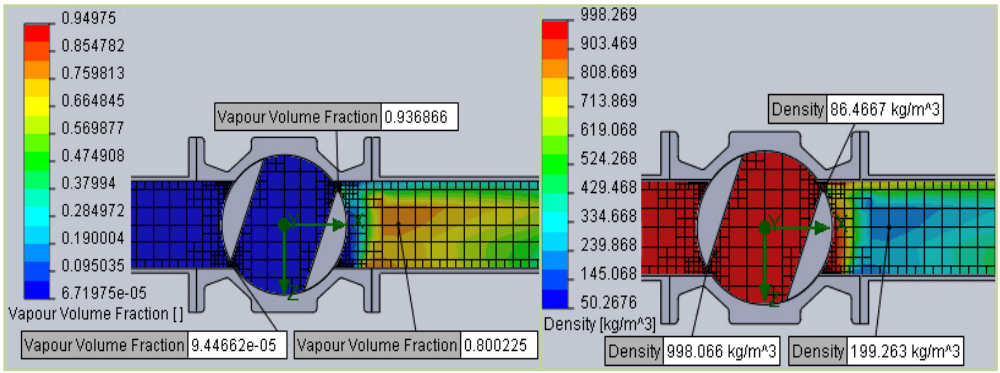

(a) (b)

Figure 5. Cavitation resulting from a ball valve opening angle of 20º - vapor volume fraction values (a) and gas-water mixture density (b) distribution values

 ©2010 International Energy & Environment Foundation. All rights reserved.

The flow through the valve results in the contraction of the liquid vein (Figure 6a) immediately upstream and downstream of the closure and therefore in the flow velocity increase in these regions. What explains the pressure decrease from the region immediately upstream of the actuator towards downstream. This pressure decrease resulting from a ball valve opening angle of 45º, but conditions for cavitation occurrence are not created. The representation of flow trajectories, Figure 6b, allows the identification of flow separation, rotational movement inside the valve and vorticity with high turbulence intensity associated, downstream of the closure.

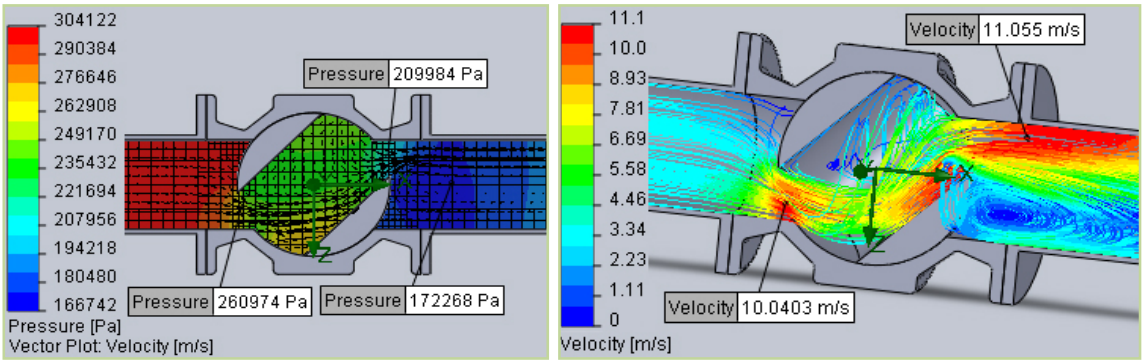

(a) (b)

Figure 6. Ball valve opening angle of 45º - velocity vector and pressure distribution (a) and flow trajectories (b) in a longitudinal section of a ball valve

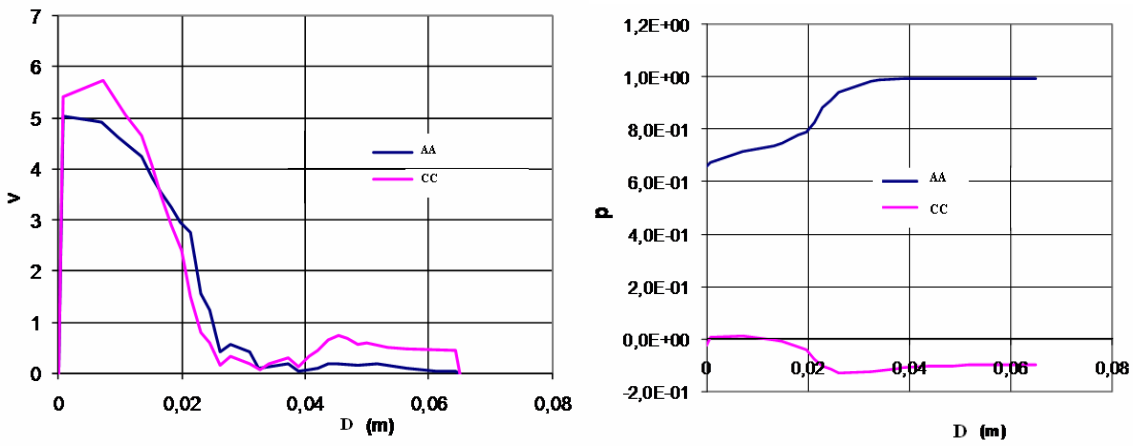

Graph 2. Ball valve opening angle of 45º - velocity (v/vo) (a) and pressure (p/po) profiles

Graph 2 shows the layout of the velocity and pressure profiles along stretches immediately upstream and downstream of the valve. For this opening, it shows the rotational flow at downstream of the valve. Due to the convergence of flow paths upstream, the flow has irrotational characteristics as is in a narrowing section.

3.1.2 Globe valve

From the 3D geometry of a globe valve were obtained the results regarding to head losses induced. From Table 2 and Graph 3 can be concluded that in the case of a globe valve the local head loss coefficient K_v value varies little with the valve opening percentage, and that this valve has higher K_v values, concerning to the fully opened valve position, than the other analyzed valves. This can be justified considering the valve geometry much more tortuous for the flow passage than the other valves geometry.

 ©2010 International Energy & Environment Foundation. All rights reserved.

Table 2. Head loss and local head loss coefficient values for different globe valve opening angles

	Percentagem de abertura da válvula de globo (%)				
	20	40	60	80	100
ΔH (m)	13,60	3,62	2,56	1,71	1,70
Kv (-)	17,25	5,69	4,48	2,82	2,81

The geometry of this valve includes curves, both upstream and downstream of the valve actuator. In the soffit of this curves there is a pressure reduction and a velocity increase. This variation is more evident in the smaller radius curves immediately upstream and downstream of the obturator (Graph 3).
The smallest radius curve located immediately downstream of the closure corresponds to a contracted flow section and downstream from it occurs an enlargement of the section that causes the velocity decrease and the flow trajectories divergence.

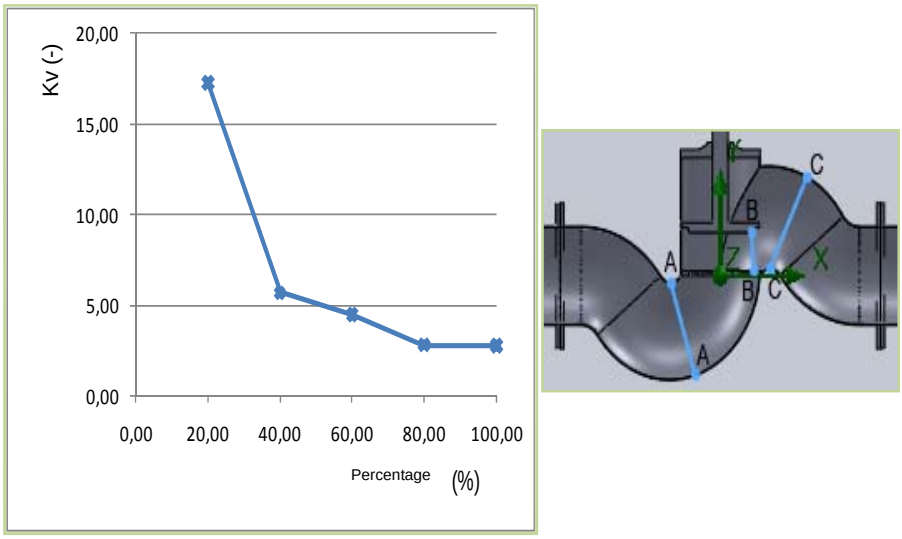

Graph 3. Globe valve - local head loss coefficient variation with the opening angle

As a result is formed a separation flow zone, where the pressure decreases giving rise to the formation of macro vorticity which justifies the energy dissipation induced into the flow due to the globe valve. In turn, this vortex locally blocks the flow section (Figure 7) which causes the flow trajectories contracting and gives rise to new flow separation and thus to energy losses. The formed vortices, which detach and disintegrate towards downstream, cause valve and pipe vibrations and give rise to turbulent wake formation. For larger valve openings the reduction in K_V values is low, which can be justified considering that the valve region where the obturator moves always occurs a decrease on pressure and velocity values for any opening degree.

 ©2010 International Energy & Environment Foundation. All rights reserved.

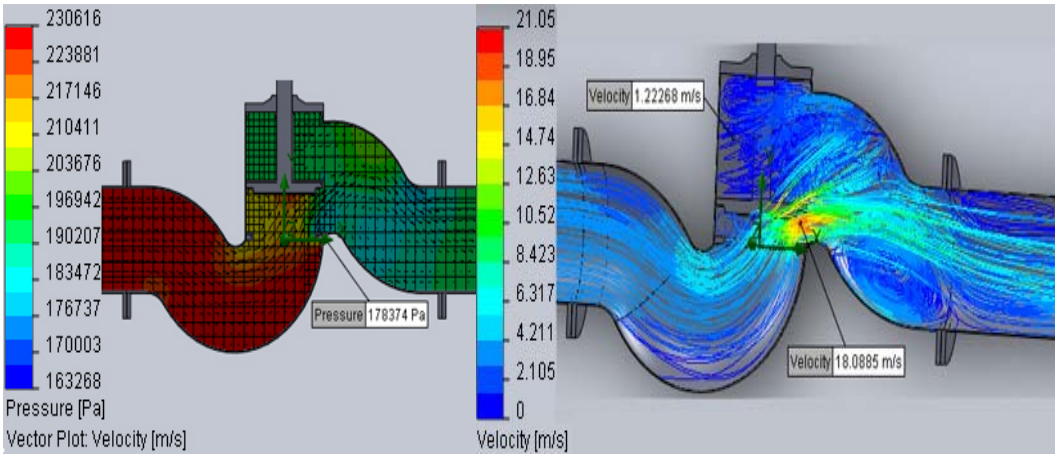

(a) (b)

Figure 7. Velocity vector and pressure distribution for an obturator opening of 40% (a) and flow trajectories (b) in a longitudinal section of a ball valve

The velocity profile at downstream shows a rapid increase in velocity values, which is due to the concavity of the external borders of the valve, which follows a rapid velocity reduction, explained by the occurrence of flow separation zone, with macro vorticity (Graph 4) with significant recirculation zone along the curvature of the outside of the outlet valve.

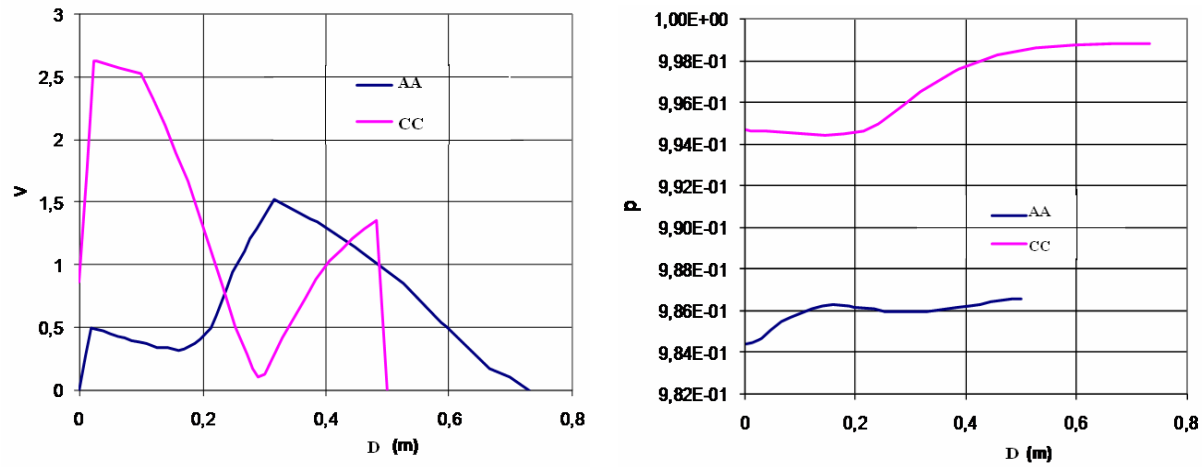

Graph 4. Globe valve: (a) velocity (v/vo) and (b) pressure (p/po) profiles

3.2 SHP intake

There are different types of intakes with diversion flow to the turbine through the penstock: frontal, lateral, bottom drop and siphon type. It is necessary to design the entrance shape in order to avoid separated zones of the flow and excessive head loss through wing walls and to verify the minimum submergence in order to avoid vortex formation and, consequently, air dragging (Figure 8).

 ©2010 International Energy & Environment Foundation. All rights reserved.

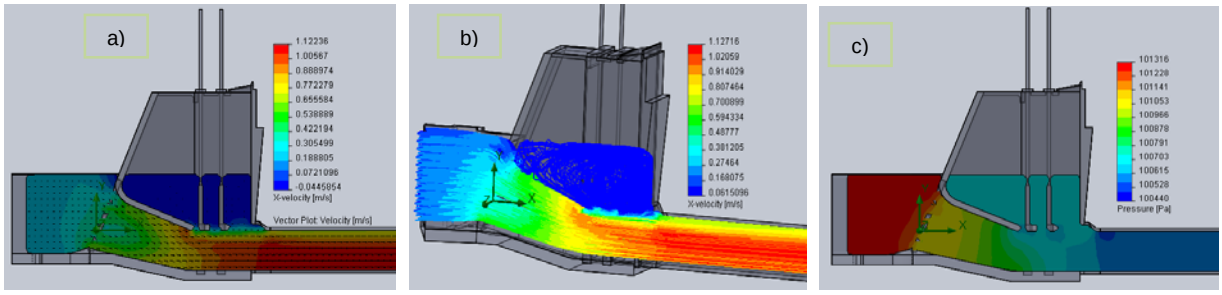

Figure 8. Improved SHP intake: (a) velocity distribution with velocity vectors; (b) streamlines; (c) static pressure distribution

The Cauchy-Rieman equations enable the velocity potential to be calculated if stream function is known resulting in the Laplace equation, verifying that streamlines and equipotential lines are mutually perpendicular originating a flow net of streamlines and equipotential lines. When the stream lines converge the velocity increases (Figure 8) and consequently distance between equipotential lines will decrease. So abrupt changes of the outer boundary must be avoided in order to avoid the separation of the streamline from the boundary.

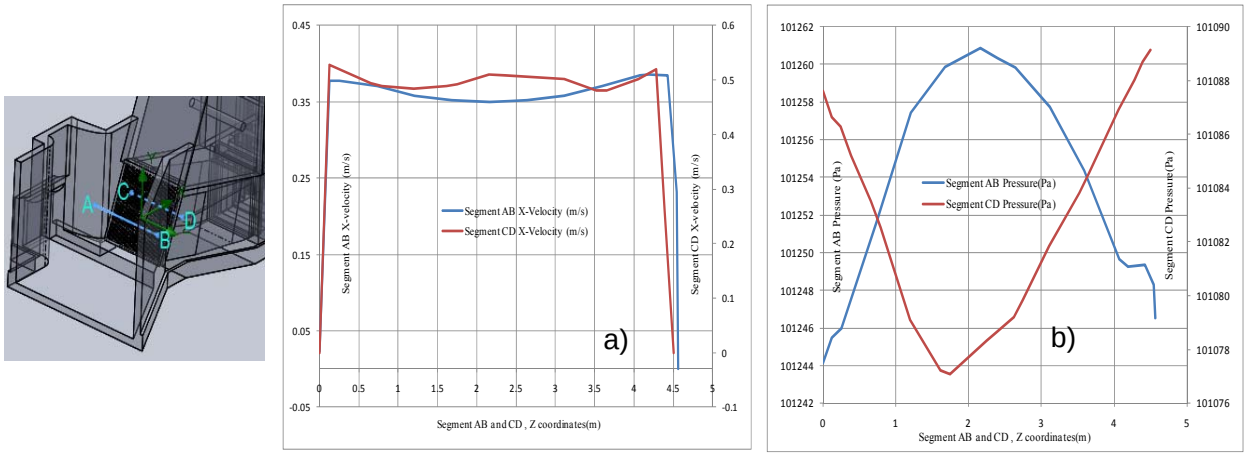

Graph 5. Velocity (a) and pressure (b) variation along the AB and CD water intake segments

In sharp boundaries the velocity at the separation volume will be zero and the fluid trapped there will be stagnant. In convergent the velocity turns away from the fluid, indicating high velocity in the separation with significant rotation. Therefore the assumption of irrotational flow is not valid there. Hence smooth converging has no separation. By analyzing Grapgh 5(a) shape, the conclusion is that the flow is turbulent at the intake entrance and downstream of the trash rack. The Graph 5b is consistent with the Figure 8c and shows the pressure loss across the trash rack.

3.3 Francis turbine

The first step is to create the geometry model, using a CAD software, of the hydraulic Francis turbine, represented in Figure 9, in order to simulate the hydrodynamic flow behavior through it. For this model were defined as boundary conditions a inlet volume flow of 6 m^3s^{-1} at the inlet and a static pressure of 121590 Pa at the outlet. For the runner angular velocity two scenarios were considered of 750 rpm and 1000 rpm.

The head loss $\Delta H\,(m)$ is determined for each scenario considering the equation (3):

 ©2010 International Energy & Environment Foundation. All rights reserved.

$$\Delta H = \frac{\left(P_{0,ups} - P_{0,dow}\right)}{\gamma} \quad (3)$$

where: $P_{0,ups}$: total pressure at upstream section (Pa); $P_{0,dow}$:total pressure at downstream section (Pa); γ : water specific weight (N/m^3).
As upstream sections the inlet model section and the inlet spiral case section were considered. As downstream sections the outlet model section, first and last draft tube bend sections were considered.

In order to determine the total pressure $P_0(Pa)$ at those sections the CFD model considers the equation (4).

$$P_0 = p + \frac{\rho U^2}{2} \quad (4)$$

where: p : static pressure (Pa); ρ : water volume mass (kg/m^3); U : average flow velocity at each section (m/s).

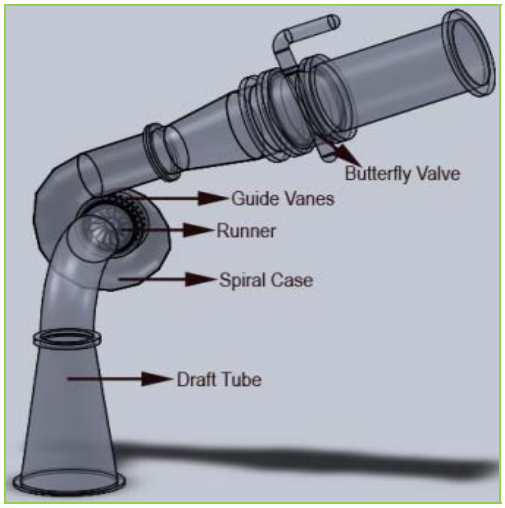

Figure 9. Francis turbine geometric model

For the first scenario of 750 rpm the following results related with the pressure head are obtained.

Table 3. Pressure Head for the scenario of 750 rpm

	Pressure Head (m)
inlet model section – outlet model section	146
inlet spiral case section - first draft tube bend section (net head)	109
inlet spiral case section - last draft tube bend	130

For the second scenario of 1000 rpm the following results related with the pressure head are obtained.

Table 4. Pressure Head for the scenario of 1000 rpm

	Pressure Head (m)
inlet model section – outlet model section	209
inlet spiral case section - first draft tube bend section (net head)	151
inlet spiral case section - last draft tube bend	186

 ©2010 International Energy & Environment Foundation. All rights reserved.

For this greater angular velocity related with the same runner geometry and the same volume flow rate the obtained pressure head values are greater, so that the turbine net head is also greater enabling greater energy production [13].

The CFD model also provides results enabling the analysis of the hydrodynamic flow parameters distribution on the model's surfaces or on sectioning planes (Figure 10).

Analyzing Figures 10 (a) and (b), the conclusion is that the velocity increases from the inlet to the runner were it reaches the maximum value, and diminish from the runner to the outlet. From the runner to the outlet the flow is rotational. At the runner outlet and the draft tube's first stretch and bend, the flow velocity at the inner part is very close to zero and increases from the inner to outer wall.

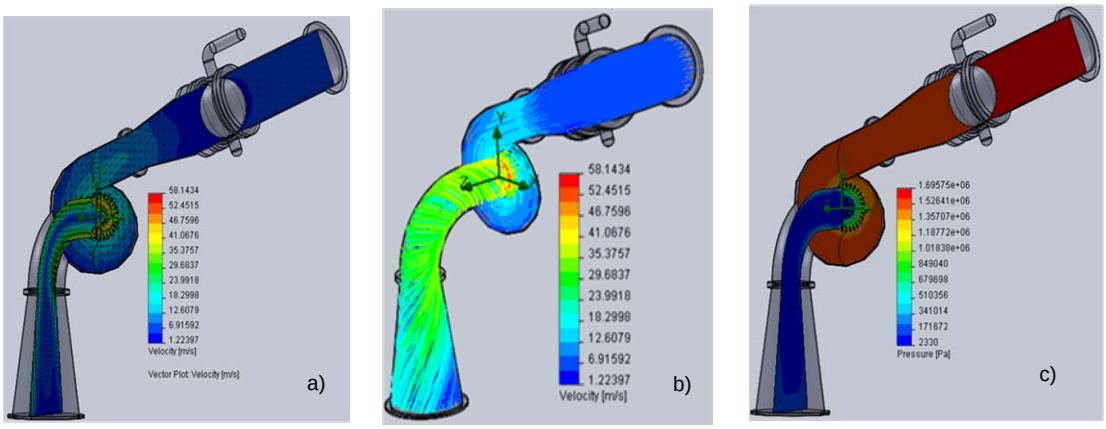

Figure 10. First scenario of 750 rpm: (a) velocity distribution with velocity vectors; (b) flow velocity trajectories; (c) static pressure distribution

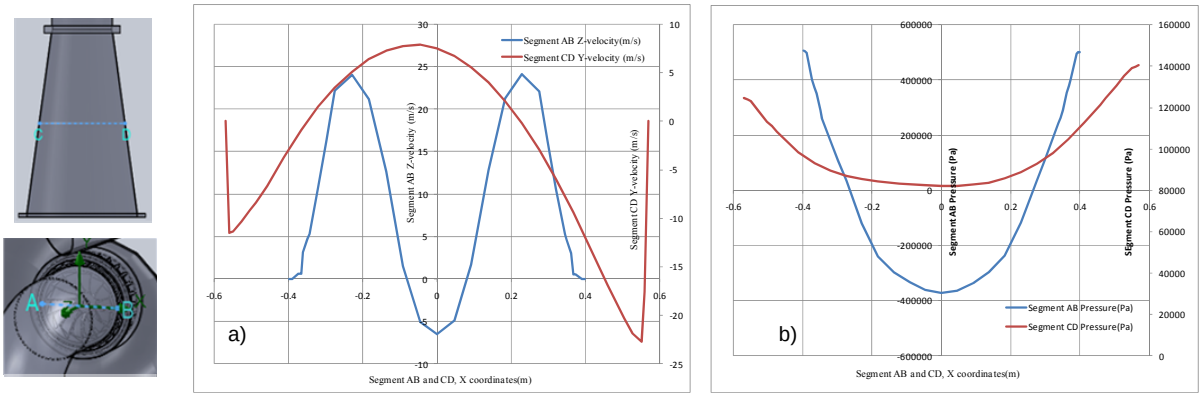

Graph 6. First scenario of 750 rpm: (a) velocity; (b) pressure variation along the AB and CD Francis turbine segments

This is in accordance with the vortex developed at the runner outlet, which can be seen by the flow velocity trajectories shape and by the flow velocity vector field. On the Figure 10c the difference between the static pressure at the sections upstream the runner and downstream the runner can be seen and justify the values obtained for the pressure head at Table 3. Analyzing the low pressure values obtained at the runner exit and at the draftube is possible to predict cavitation for this flow conditions [14].

Analyzing Graph 6, at the runner outlet (segment AB) both the velocity and the pressure decreases from the periphery to the center of the segment. This shows that here the flow is rotational. However, unlike the pressure values, the velocity values decreases towards the periphery, providing flow separation, thus

 ©2010 International Energy & Environment Foundation. All rights reserved.

at this segment periphery the flow is irrotational. At the segment's CD ends the velocity values are negative, thus the water flows towards the exit (given the y-axis direction). However at the segment's CD center the velocity values are positive thus the flow enters the model. This shows that there is a vortex at the draft tube's diffuser which can be consider a reverse flow zone. This is in accordance with the flow velocity trajectories shape and with the flow velocity vector field.

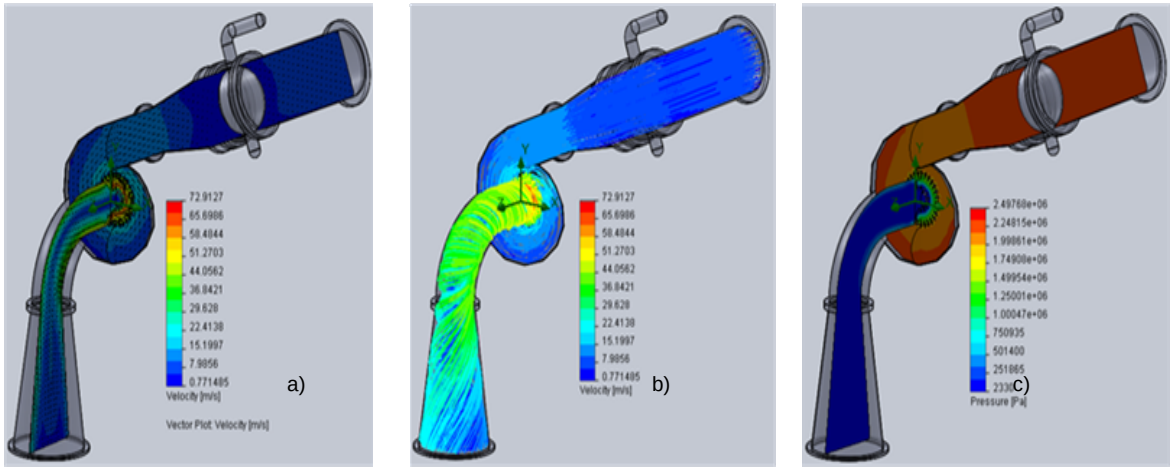

Figure 11. Second scenario of 1000 rpm: (a) velocity distribution with velocity vectors; (b) flow velocity trajectories; (c) static pressure distribution

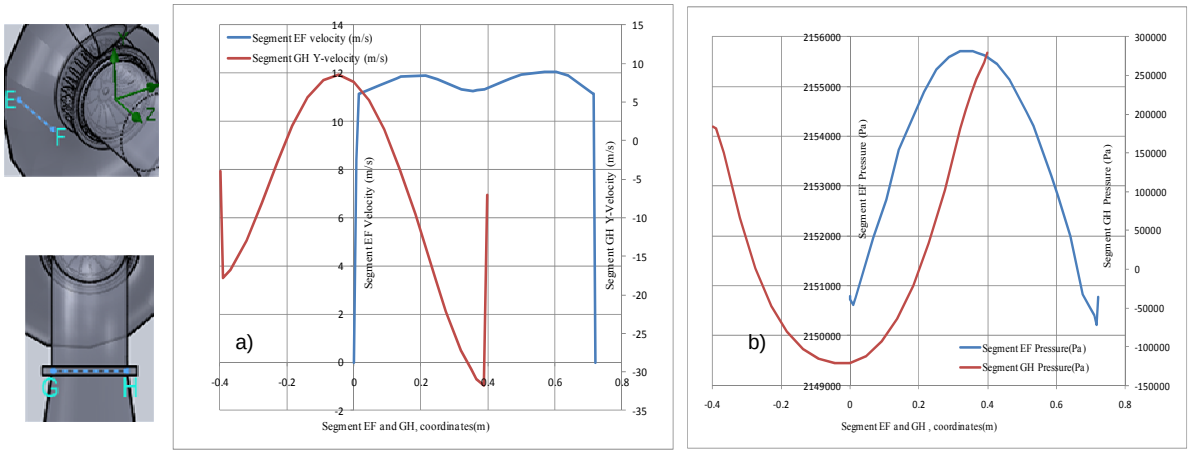

Graph 7. Second scenario of 1000 rpm: (a) velocity; (b) pressure variation along the EF and GH Francis turbine segments

Analyzing Figures 11 (a) and (b), the conclusions are quite similar to the previous, but in this case the flow velocity on the runner and the pressure head are even greater. The vortex formed at the inner part, from the runner outlet to the model outlet, is in this scenario, even more intense and occupies more space, leading to greater head losses as a result of vortex turbulence. The pressure gradient which is observed at Figure 11b is in accordance with the values obtained on Table 4 and the lower pressure values indicate the cavitation occurrence.

The velocity variation at spiral case segment EF (Graph 7) shows that the flow is turbulent. The velocity values increase from the outer wall towards the inner space where the flow direction changes, and the water flows from the model outlet to the draft tube's first stretch, being a reverse flow region.

 ©2010 International Energy & Environment Foundation. All rights reserved.

3.4 Francis turbine outlet and tailrace

CFD model has been applied to simulate the highly turbulent flow conditions in turbine and tailrace region, since there are important parts of a hydropower facility that carries water away from the turbines. This analysis is used to study operational and structural possible modifications that could improve the hydrodynamic behavior for different flow and hydromechanical conditions. Critical depths, suction heads and the volume rate of flow can be identified and avoided since such occurrence are limiting factors for a good design, with strongly influence in the hydro systems efficiency.

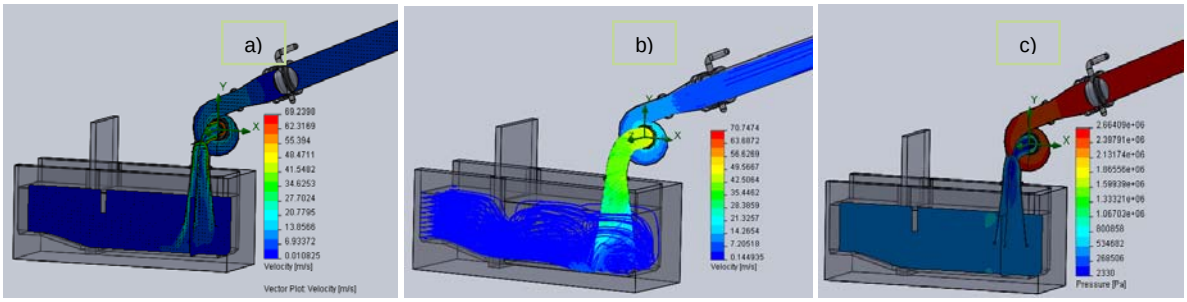

Figure 12. Turbine and tailrace: (a) velocity distribution with velocity vectors; (b) streamlines; (c) static pressure distribution

Shear stresses are developed when the fluid is in motion, when the particles move relative to each other with different velocities or when the fluid is in contact with a solid boundary. In Figure 12 is visible, due to fluid rotation, a vortex motion in the draft tube where the streamlines form a set of concentric circles and there is a change of total pressure or energy.

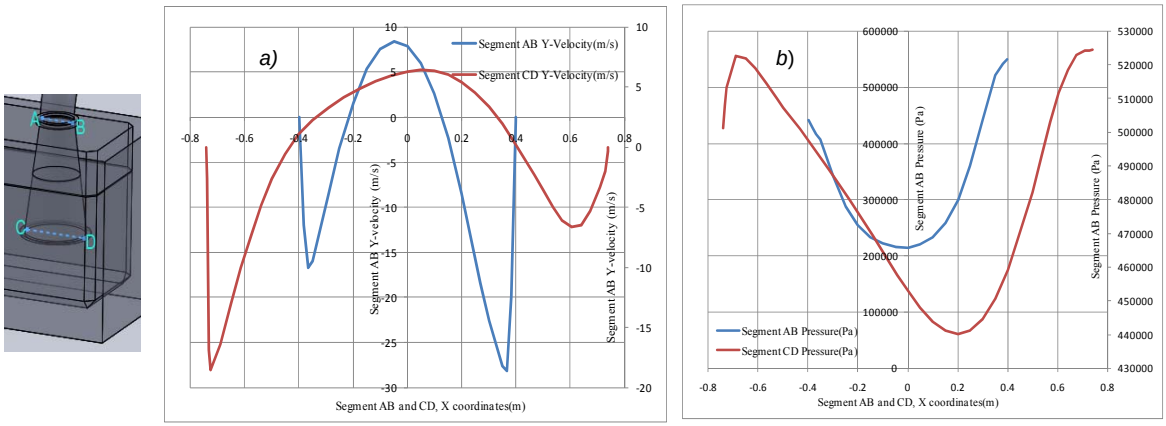

Graph 8. Turbine outlet and tailrace: (a) velocity; (b) pressure variation along the AB and CD segments

In Graph 8 the inversion of the flow velocity in the middle of the draft tube enhance the inversion of the flow due to the influence of the rotational speed and the pressure reduction in that middle zone, confirming the rotational flow type. The influence of the design in the tailrace is quite important in terms of with, length and depth, position of the gate and the uplift of the sill making the transition into the river.

4. Conclusions

The advanced CFD model used in this research (FloEFD) solves the Navier-Stokes equations, which are formulations of mass, momentum and energy conservation laws for fluid flows. This CFD model is able of predicting both laminar and turbulent flows. Most of the fluid flows in engineering practice are turbulent, so this model uses the Favre-averaged Navier-Stokes equations, where time-averaged effects of the flow turbulence on the flow parameters are considered, whereas the other, i.e. large-scale, time-

 ©2010 International Energy & Environment Foundation. All rights reserved.

dependent phenomena are taken into account directly. Through this procedure, extra terms known as the Reynolds stresses appear in the equations for which additional information must be provided. To close this system of equations, FloEFD employs transport equations for the turbulent kinetic energy and its dissipation rate, the so-called *k*-ε model.

This paper shows the utility of the CFD numerical simulations as a tool for design and optimization of hydropower performance and flow behavior through hydromechanical devices or hydraulic structures of intake and outlet types. Experimental tests not always are viable because they are very expensive and it is much more difficult to analyze different scenarios and boundaries.

The flow of a real fluid in contact with a boundary implies velocity variations, pressures gradients and shear stress development, from which energy losses result, as important factors to take into account in the concept, design, construction, operation and maintenance of hydropower plants or any other type of hydraulic conveyance system.

Acknowledgements

To projects HYLOW from 7th Framework Programme (Grant nº 212423) and FCT (PTDC/ECM/65731/2006) and (PTDC/ECM/68694/2006) which contributed to the development of this research work in the domain of computational dynamic analyses.

References

[1] Ramos, H., Non conventional dynamic effects in Pressurised hydraulic systems. Elements to support the course Unsteady Flows and Hydropower and Pumping Systems of Hydraulic MSc Course. IST, DECivil, 2004, (in Portuguese).

[2] Ramos, H., Guidelines for Design of Small Hydropower Plants. Book published by WREAN (Western Regional Energy Agency and Network) and DED (Department of Economic Development - Energy Division). Total pp 205. Belfast, North Ireland. ISBN 972-96346-4-5, 2000.

[3] Ruprecht, A., Eisinger R., Göde, E.: Innovative Design Environments for Hydro Turbine Components, Bern, HYDRO 2000, 2000

[4] Ramos, H., Hydropower and Pumping Systems. MSc of Hydraulic and Water Resources. IST, DECivil, 2003, (in Portuguese).

[5] Douglas, J.F. Gasiorek, J.M., Swaffield, J.A., Fluid Mechanics. 3rd Edition, Longman Group Limited, 1998.

[6] Visser, F.C., Brouwers, J.J.H., Jonker, J.B., Fluid flow in a rotating low-specific-speed centrifugal impeller passage. J. Fluid Dynamics Research, 24, pp. 275-292, 1999.

[7] MENTOR GRAPHICS, FloEFD - Technical Reference, (EUA), 2008.

[8] Lipej, A., Poloni, C.: Design of Kaplan Runner Using Multiobjective genetic algorithm optimization, Journal of Hydraulic Research, Vol. 38, 2000.

[9] Mrsa, Z., Sopta, L., Vukovic, S.: Shape optimization method for Francis turbine spiral casing design, ECCOMAS, Athen, 1998.

[10] Ramos, H. and Almeida, A. B., Parametric Analysis of Waterhammer Effects in Small Hydropower Schemes. HY/1999/021354. ASCE - Journal of Hydraulic Engineering. Volume 128, 7, pp. 689-697, ISSN 0733-9429, 2002.

[11] Ramos, H; Almeida, A. B., Dynamic orifice model on waterhammer analysis of high and medium heads of small hydropower schemes. Journal of Hydraulic Research, IAHR, Vol. 39 (4), pp. 429-436, ISSN-0022-1686, 2001.

[12] Pereira, A., Ramos, H.M., Hydrodynamic analyses in water conveyance components, IX SEREA - Seminario Iberoamericano sobre Planificación, Proyecto y Operación de Sistemas de Abastecimiento de Agua. Valencia (España), 24-27 de Noviembre de 2009, (in Portuguese).

[13] Skot´ak A.: The CFD Prediction of the Dynamic Behavior of Pump-Turbine, Proc. 11th IAHR WG1 meeting, Stuttgart, 2003.

[14] Backman A.G.: CFD Validation of Pressure Fluctuations in a Pump Turbine, Master's Thesis, TU Luela, 2008.

 ©2010 International Energy & Environment Foundation. All rights reserved.

Ana Pereira is in his final year of Civil Engineer MSc at Instituto Superior Técnico (Technical University of Lisbon – Portugal) and has few publications. She is researcher under the scientific domain of water and energy, CFD for SHP and participates in the FCT Project - PTDC/ECM/68694/2006 – Vulnerability and behaviour of hydraulic conveyance systems.
E-mail address: cardper@gmail.com

Helena M. Ramos has Ph.D. degree with the Aggregation Title and she is Professor at Instituto Superior Técnico (from Technical University of Lisbon - Portugal) at Department of Civil Engineering. Expert in different scientific domains: Hydraulics, Hydrotransients, Hydropower, Pumping Systems, Leakage Control, Energy Efficiency and Renewable Energy Sources, Water Supply, Vulnerability. More than 250 publications being 1 book in Small Hydro, 52 in Journals with referee and 110 in International Conferences; Supervisor of several post-doc, PhDs and MSc students and author of 8 innovative real solutions in the domain of Civil Engineering - hydropower and hydraulic system control.
E-mail address: hr@civil.ist.utl.pt or hramos.ist@gmail.com

ISSN 2076-2895 (Print), ISSN 2076-2909 (Online) *©2010 International Energy & Environment Foundation. All rights reserved.*